ARL-TN-0908 ● SEP 2018

US Army Research Laboratory

Heat Loss in a Micro-Combustion Chamber

by Steven W Dean, Jeffrey B Morris, and Jennifer L Gottfried

NOTICES

Disclaimers

The findings in this report are not to be construed as an official Department of the Army position unless so designated by other authorized documents.

Citation of manufacturer’s or trade names does not constitute an official endorsement or approval of the use thereof.

Destroy this report when it is no longer needed. Do not return it to the originator.

ARL-TN-0908 ● SEP 2018

US Army Research Laboratory

Heat Loss in a Micro-Combustion Chamber

by Steven W Dean, Jeffrey B Morris, and Jennifer L Gottfried
Weapons and Materials Research Directorate, ARL

REPORT DOCUMENTATION PAGE

Form Approved
OMB No. 0704-0188

1. REPORT DATE *(DD-MM-YYYY)*	2. REPORT TYPE	3. DATES COVERED (From - To)
September 2018	Technical Note	January 2018–July 2018

4. TITLE AND SUBTITLE
Heat Loss in a Micro-Combustion Chamber

5a. CONTRACT NUMBER

5b. GRANT NUMBER

5c. PROGRAM ELEMENT NUMBER

6. AUTHOR(S)
Steven W Dean, Jeffrey B Morris, and Jennifer L Gottfried

5d. PROJECT NUMBER

5e. TASK NUMBER

5f. WORK UNIT NUMBER

7. PERFORMING ORGANIZATION NAME(S) AND ADDRESS(ES)
US Army Research Laboratory
ATTN: RDRL-WML-B
Aberdeen Proving Ground, MD 21005

8. PERFORMING ORGANIZATION REPORT NUMBER
ARL-TN-0908

9. SPONSORING/MONITORING AGENCY NAME(S) AND ADDRESS(ES)

10. SPONSOR/MONITOR'S ACRONYM(S)

11. SPONSOR/MONITOR'S REPORT NUMBER(S)

12. DISTRIBUTION/AVAILABILITY STATEMENT
Approved for public release; distribution is unlimited.

13. SUPPLEMENTARY NOTES

14. ABSTRACT
Previous preliminary work to assess the viability of a laboratory-scale confined laser ignition chamber with a capacity of 0.500 cm^3 as a micro-combustion bomb did not take into account corrections for heat loss. In this report, we address pressure corrections to account for radiative and convective heat loss for M10, JA2, WC450, and CL20. Our attempt to correct for heat loss with a dry blend of WC450 and CL20 was not successful.

15. SUBJECT TERMS
laser ignition, propellant, impetus, micro-combustion bomb, M10 propellant, JA2 propellant, CL20, WC450 ball propellant

16. SECURITY CLASSIFICATION OF:			17. LIMITATION OF ABSTRACT	18. NUMBER OF PAGES	19a. NAME OF RESPONSIBLE PERSON
a. REPORT	b. ABSTRACT	c. THIS PAGE			19b. TELEPHONE NUMBER (Include area code)
Unclassified	Unclassified	Unclassified	UU	17	Steven W Dean (410) 278-6357

Contents

List of Figures

List of Tables

Acknowledgments

The authors gratefully acknowledge Kevin Bare for preparation and delivery of propellant samples used in this report.

1. Introduction

In ARL-MR-0972 we described the use of a laboratory-scale combustion chamber with an internal capacity of 0.500 cm^3 to estimate impetus at low loading densities.[1] Our work in that report found a strong linear relationship between the measured impetus for samples of Class-3 black powder, JA2, and M10 propellants against their corresponding reference values. While the correlation was linear, the experimental values were significantly low compared to their reference values. We concluded there were significant nonadiabatic heat losses in the chamber due to the high surface-area-to-volume ratio relative to larger combustion chambers with at least 25 cm^3 capacities. The low loading densities supported an ideal gas treatment as opposed to the traditional Noble–Abel treatment that takes into account co-volume. While extremely nonadiabatic, the strong linear correlation supports a heat loss mechanism that results in a constant percentage reduction in final pressure across all of the samples studied. In this report we consider the effects of radiative and convective heat loss on experimentally determined impetus measurements using this chamber.

2. Experimental

Our laser ignition experiments have been described at length in Morris et al.[1] as well as by Gottfried et al.[2] We refer the reader to those reports for specific experimental details.

In addition to the pressure–time (P-t) data mentioned in Morris et al.[1] for JA2, M10, and black powder, during the early part of FY18 we measured additional P-t data for CL20, WC450 (Saint Marks Powder) undeterred ball powder, and a 50:50 mixture of CL20/WC450. Sample mass information is provided in Table 1. Only three replicates were conducted for CL20 since each experiment resulted in pitting on the interior surface of a laser window. Form factors for each sample were as follows: CL20: fine powder; WC450 ball powder; JA2 and M10: 5- × 5-mm slab of variable thickness (nominally 1 mm thick).

Table 1 Sample mass loading for experiments with CL20 and WC450

Sample	Mass range (mg)	Average mass (mg)	No. of experiments
CL20	19.3–30.7	26.4	3
WC450	12.0–51.2	30.4	6
CL20/WC450[a]	24.5–43.8	32.8	5

[a] 50:50 ratio by mass

3. Results and Discussion

3.1 Correction for Pressure Drop Due to Radiative Heat Loss

Data analysis was done within the Microsoft Excel spreadsheet program that is part of the Microsoft Office Professional Plus 2013 software suite on a Windows-based PC. The raw data from the amplifier was in volts, calibrated to 1 V = 1,000 psi, and converted to pressure units of megapascals (MPa) within each spreadsheet. Figure 1 shows a typical pressure–time trace for WC450, with a graphical depiction of the analysis used to determine pressure correction due to radiative heat loss. The data saved with the timebase of 10 ms/division on the oscilloscope resulted in a temporal resolution of 0.1 ms. The full data trace spans a temporal range of –10 ms to +90 ms. The 100 points prior to t = 0 were averaged for a baseline adjustment.

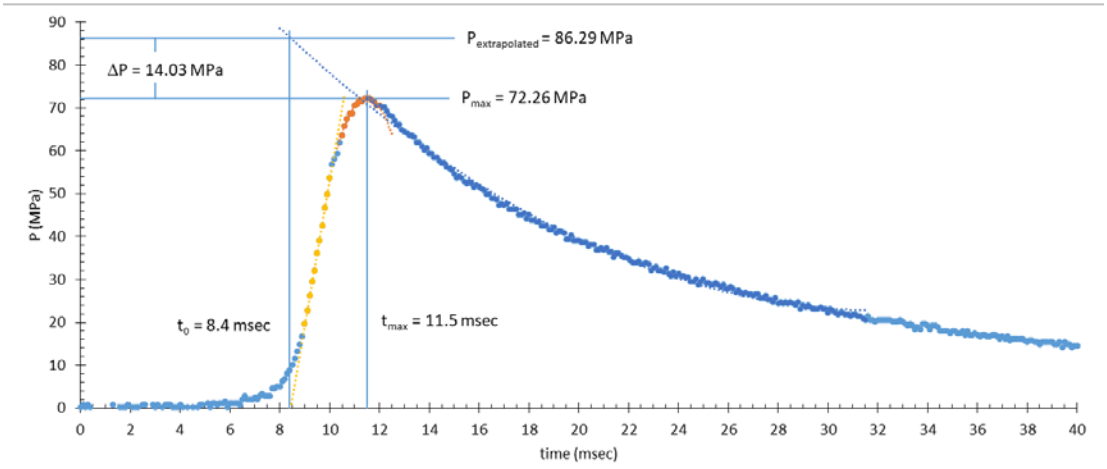

Fig. 1 P-t trace for WC450 undeterred ball powder, 51.212 mg. The figure provides a graphical representation of the estimation of ΔP used to account for pressure drop due to radiative heat loss during combustion of the propellant.

The portion of the trace to the right of the peak pressure represents pressure drop due to radiative cooling of the propellant combustion gasses past the point of propellant burnout in the chamber. The pressure drop should be in accordance with the Stefan–Boltzman law for energy transfer by radiative heat loss:

$$W = \varepsilon\sigma A(T^4 - T_c^4)\,, \qquad (1)$$

where W = net radiated power (J/s); ε = emissivity; σ = Stefan–Boltzman constant; A = surface area; T = absolute temperature of the hot object (in this case the burning propellant and combustion gases); and T_c = absolute temperature of the colder surrounding (in this case the combustion chamber). As $T^4 >> T_c^4$, Eq. 1 can be reduced to

$$W \cong \varepsilon\sigma A T^4 . \quad (2)$$

W represents the instantaneous rate of heat loss in terms of heat per unit time and has a strong dependence upon temperature of the combustion products.

In this experiment, we used the pressure trace following burnout of our sample as a representation of temperature using an ideal gas proportionality treatment of pressure and temperature. We did this as our experiment operated under constant volume conditions with conservation of mass between the propellant sample and combustion products. In making this proportionality assumption, we worked directly in the pressure domain to determine an approximate pressure correction, ΔP, to account for pressure drop due to radiative heat loss during combustion of the propellant.

Referring to Fig. 1, we started with the baseline-corrected pressure trace. As was done in our previous report,[1] we determined the time of maximum pressure (P_{max}) by fitting the data around P_{max} to a quadratic function and solving for the time (t_{max}) at which the slope is 0. Heat loss during combustion will have a component due to radiative heat loss and a component due to convective heat loss. Our radiative pressure correction, ΔP, will involve extrapolation of the pressure trace back to the combustion onset time, t_0. The combustion onset time is determined by extrapolating the linear portion of the pressure rise to the time axis, where $P = 0$, and noting the time at the intercept. The 200 data points in the P-t trace following P_{max} are fit to a quadratic function and extrapolated back to t_0 to determine $P_{extrapolated}$. ΔP is the difference between $P_{extrapolated}$ and P_{max}. ΔP is not the true radiative heat-loss pressure correction but needs to be adjusted with a scaling factor that accounts for the situation of a finite burning time between t_0 and t_{max}, such that the pressure correction would normally be expected to be somewhat smaller than ΔP as measured in Fig. 1.

Hunt notes the radiative heat loss will be almost proportional to the time of burning.[3] We account for burning time as the difference between t_{max} and t_0:

$$t_{burn} = t_{max} - t_0 . \quad (3)$$

We account for the pressure drop due to radiative heat loss as

$$\Delta P_{rad} = s_1 \Delta P t_{burn} , \quad (4)$$

where s_1 is an empirically determined universal scaling factor for the chamber.

3.2 Correction for Pressure Drop Due to Convective Heat Loss

Regarding convection, Hunt notes convective heat loss should result in a pressure drop that is a constant percentage for all propellants.[3] We account for the pressure drop due to conductive heat loss as

$$\Delta P_{conv} = s_2 P_{max} , \tag{5}$$

where s_2 is an empirically determined universal scaling factor for the chamber.

3.3 Determination of Scaling Factors

The corrected pressure is given by the following equation:

$$P_{corr} = P_{max} + \Delta P_{rad} + \Delta P_{conv} = P_{max} + s_1 \Delta P t_{burn} + s_2 P_{max} . \tag{6}$$

For each individual experiment with the five samples, the corrected pressure from Eq. 6 is divided by the loading density (L) to arrive at an experimentally determined impetus (F):

$$F_{experimental} = P_{corr}/L . \tag{7}$$

The scaling factors s_1 and s_2 are empirically determined by manually adjusting each factor to minimize the root mean square (RMS) difference between the value of $F_{experimental}$ and the reference value of F calculated using the Cheetah code[4] at a standard L = 0.2 g/cm^3. We used only the data for WC450 and JA2. There were six replicates for each sample spanning a collective range of L = 0.035–0.100 g/cm^3. The other data points—for M10, CL20, and the CL20/WC450 mix—were excluded in the calibration of s_1 and s_2 since we wanted to see how well data with impetus values beyond the range of WC450 and JA2 would fit the calibration.

The calibration of the chamber scaling factors was started by setting $s_2 = 0.4$ and adjusting s_1 upwards from 0 to minimize the RMS difference in the impetus values. Adjustments were made in an iterative manner between s_1 and s_2 while increasing the number of significant figures in these two scaling factors to three figures. Scaling factors for the best fit of the WC450 and JA2 data were determined to be $s_1 = 63.5\ s^{-1}$ and $s_2 = 0.395$.

3.4 Correlation of Impetus to Reference Values

Figure 2 shows the experimentally determined impetus values as individual data points plotted against calculated reference values for M10, WC450, JA2, CL20/WC450, and CL20. A solid line with slope = 1 is included in Fig. 2 as a visual

reference. In Table 2 we compare the mean experimental impetus values to the reference values and provide some statistics like percent deviation and the error bars at a 95% confidence limit. As expected, the experimental mean values for JA2 and WC450 are in good agreement with their reference values. M10 also shows excellent agreement. The close agreement of M10 to the reference value is not surprising when the chemistry of the three propellants is considered: all are nitrocellulose single- or double-base propellants.

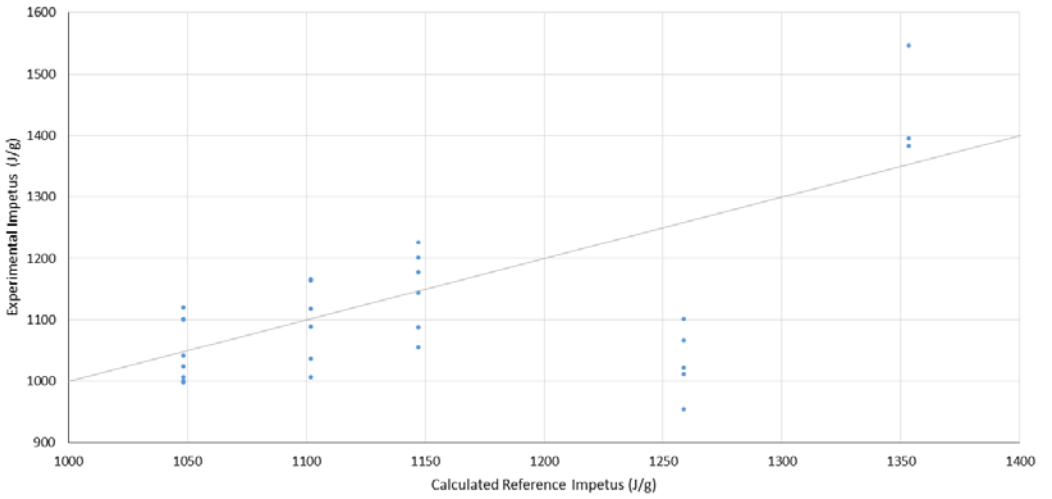

Fig. 2 Experimentally determined impetus values plotted against calculated reference values at standard loading density of 0.2 g/cm^3. From left to right, the data sets are M10, WC450, JA2, CL20/WC450, and CL20. Scaling factors used are s_1 = 63.5 s^{-1}; s_2 = 0.395.

Table 2 Experimental impetus values and statistics

Sample	Reference F (J/g)	Experimental F (J/g), mean	ΔF (%)	Error bars (J/g)	Experiments
CL20	1353	1441	+6.5	225	3
WC450/CL20	1259	1032	–18	69	5
JA2[a]	1147	1149	+0.1	70	6
WC450 [a]	1102	1097	–0.5	69	6
M10	1048	1049	+0.1	42	8

[a] Calibration data

CL20 shows reasonable agreement with its reference impetus value. Two of the CL20 experiments exhibited a hangfire delay of over 100 ms, but once combustion started, t_{burn} was very fast, less than 1 ms for all three replicates. Experimental impetus values for two of the CL20 data points are very close to the reference value, with the third data point showing a large separation from the other points. The mixture of WC450 and CL20 will be discussed in the following subsection of this report. The error bars for each sample are consistent with the number of experiments and the spread in the data.

3.5 WC450/CL20 Dry Blend

Figure 3 shows the pressure–time trace for a WC450/CL20 dry blend used in this study. Comparison with Fig. 1 shows a significant difference in the shape of the pressure rise prior to P_{max}. As with the burning of CL20, we see a steep pressure rise lasting less than 1 ms. At t = 4 ms, we see a break in the rate of pressurization (i.e., a change in the slope) as the CL20 has been consumed. The net effect is that the CL20 has prepressurized the chamber for combustion of the WC450. There is a change in pressurization mechanism relative to the neat CL20 and the formulated propellants. It would not be surprising if this change in mechanism affects both the rates of radiative and convective heat loss, and may very well be the reason for the poor correlation seen between experimental and reference impetus for this mix.

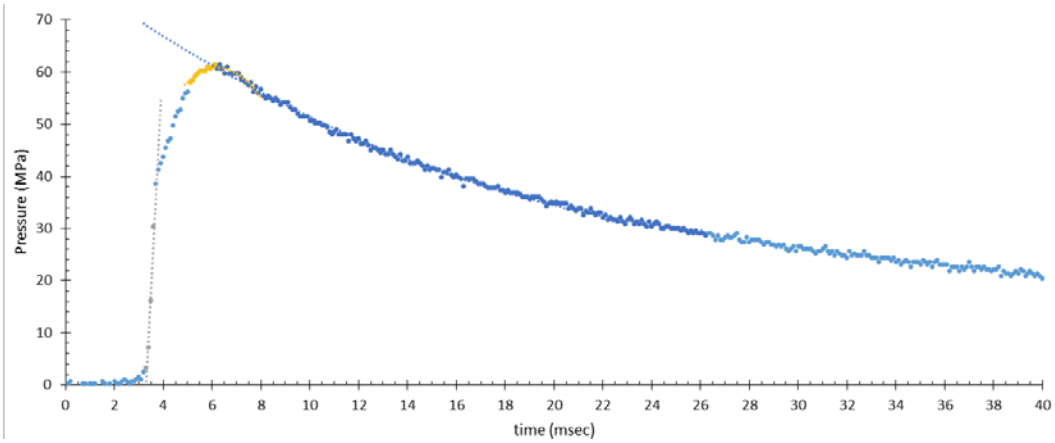

Fig. 3 P-t trace for 50:50 mix WC450/CL20, 43.764 mg total mass

We specifically added this mix to provide a sample with impetus between that of CL20 and JA2. It is possible a formulated mix that resembles CL20 distributed throughout a "WC450 binder" would have a P-t trace similar to the other formulated samples, with an experimental impetus more in line with the calculated reference value. We had also considered adding cellulose acetate/butyrate (CAB) as a dry blend to WC450 to produce samples with lower impetus values. We expected a similar result for the CAB/WC450 mix as we have seen for WC450/CL20, with the WC450 combusting first and the CAB—being inert—perhaps not combusting at all in an unformulated dry blend.

An interesting observation coming out of the work with WC450 and CL20 is that the onset of combustion for the mix is faster than either of the individual components.

4. Conclusion

In this report, we addressed heat loss in a micro-combustion chamber. CL20, WC450, JA2, and M10 are all clean-burning energetic materials leaving little to no residue after combustion. Through the application of concepts to address heat loss in larger closed bombs, we have addressed, to some degree, the pressure drop in the observed P-t trace due to radiative and convective heat loss. We were able to correct pressures using an empirical approach for nitrocellulose-based propellants. The approach worked reasonably well for CL20, although the sample size was limited due to combustion of neat CL20 being destructive to the interior face of our fused silica pressure windows.

The use of a dry blend of CL20 and WC450 to add a data point at an intermediate impetus value between that of CL20 and JA2 did not work well. Based on the form of the P-t trace, it appeared the CL20 and WC450 burned independently and sequentially, with the CL20 being consumed before much, if any, of the WC450 started to combust. This resulted in a poor correlation between calculated and experimentally determined impetus for this mix, due to a change in the mean rates of convective and radiative heat loss midburn. We also believe a fully mixed and extruded propellant with the same overall composition might provide a different result more in line with what we expected.

5. References

1. Morris JB, Dean SW, Gottfried JL. Use of a laboratory-scale confined laser ignition chamber as a micro-combustion bomb to estimate impetus at low loading density. Aberdeen Proving Ground (MD): Army Research Laboratory (US); 2018 Feb. Report No.: ARL-MR-0972.

2. Gottfried, JL, Munson CA, Colburn J, Beyer A. Initial testing of a prototype laser ignition chamber. Aberdeen Proving Ground (MD): Army Research Laboratory (US); 2014 March. Report No.: ARL-TR-6862.

3. Hunt FRW, editor. Internal Ballistics. New York (NY): The Philosophical Library, Inc.; 1951. Chapter V, Combustion at constant volume.

4. Bastea S, Fried LE, Glaesemann KR, Howard WM, Kuo I-FW, Souers PC, Vitello PA. CHEETAH v8.0 thermochemical code. Livermore (CA): Energetic Materials Center, Lawrence Livermore National Laboratory; 2015.

List of Symbols, Abbreviations, and Acronyms

ε	emissivity
σ	Stefan–Boltzman constant
CAB	cellulose acetate/butyrate
F	impetus
L	loading density
P-t	pressure–time
RMS	root mean square
T	absolute temperature
W	net radiated power

1 (PDF) DEFENSE TECHNICAL INFORMATION CTR DTIC OCA

2 (PDF) DIR ARL
IMAL HRA
RECORDS MGMT
RDRL DCL
TECH LIB

1 (PDF) GOVT PRINTG OFC
A MALHOTRA

15 (PDF) ARL
RDRL WML B
S W DEAN
J L GOTTFRIED
E F BYRD
A PESCE-RODRIGUE
K L BARE
N J TRIVEDI
RDRL WML C
K L MCNESBY
C A MUNSON
RDRL WML D
R A BEYER
J W COLBURN
J CONROY
S L HOWARD
M J MCQUAID
RDRL WMP G
B E HOMAN
RDRL WMS
J A CIEZAK-JENKINS